PHYSICSAccess Research Paper
ISSN Online: 2756-3898, ISSN Print: 2714-500X https://doi.org/10.47514/phyaccess.2026.6.1.006

Bandwidth Enhancement in White LED Visible Light Communication Systems Using Blue Optical Filtering and Multi-Stage Equalization

Abdurrasheed B Magaji[1], and Shariff M Abdulkadir[2]

[1] Department of Physics, Faculty of Natural and Applied Sciences, Umaru Musa Yar'adua University, Katsina, Katsina State, Nigeria
[2] Department of Physics, Federal College of Education, Katsina, Katsina State, Nigeria

Corresponding E-mail: abdulrasheed.magaji@umyu.edu.ng

Received 19-01-2026
Accepted for publication 20-02-2026
Published 23-02-2026

Abstract

Visible Light Communication (VLC) enables short-range high-speed data transmission using white light-emitting diodes (LEDs) for both illumination and communication. However, phosphor-converted white LEDs suffer from limited modulation bandwidth due to slow phosphor relaxation dynamics, resulting in signal attenuation, inter-symbol interference (ISI), and degradation of signal-to-noise ratio (SNR) at higher frequencies. In this work, performance enhancement using blue optical filtering combined with electrical equalization was experimentally investigated for phosphor-converted white LEDs transmitting On-Off Keying Non-Return-to-Zero (OOK-NRZ) signals. Measurements were conducted over a 40 cm indoor line-of-sight link with data rates varied from 0.5 to 20 Mbps. Two equalizer configurations were evaluated: a single-stage RC network (EQ1) and a three-stage cascaded RC network (EQ2). Frequency sweep measurements (representing OOK symbol rate variation) were performed to evaluate received signal strength, SNR, Bit Error Rate (BER), cumulative signal improvement, and normalized performance metrics. Results show that EQ2 provides significantly superior performance compared to EQ1, achieving a peak SNR of 34 dB at 10 Mbps with a corresponding BER reduction to 10^{-9}, representing approximately 8 dB SNR improvement over EQ1 at the optimal frequency. The optimal enhancement region for EQ2 lies between 0.5 and 12 MHz, where LED channel attenuation is most dominant. Polynomial fitting was used as an empirical approximation, with fifth-order models providing the highest regression accuracy for EQ2 ($R^2 = 0.90$). The results demonstrate that the combination of blue optical filtering and multi-stage equalization effectively mitigates LED bandwidth limitations, significantly improving VLC performance for indoor smart lighting and short-range wireless applications.

Keywords: Visible Light Communication (VLC); Phosphor-Converted White LED; Blue Optical Filtering; Multi-Stage Equalization; Modulation Bandwidth Enhancement; OOK-NRZ Modulation; Signal-to-Noise Ratio; Bit Error Rate.

I. INTRODUCTION

Visible Light Communication (VLC) has gained attention as a complementary wireless technology capable of meeting the increasing data rate demands imposed by smart homes, Internet of Things (IoT), and indoor networking systems [1–4]. VLC utilizes the visible optical spectrum (380–780 nm) for communication, offering advantages such as electromagnetic interference immunity, enhanced security, and dual-function illumination and data transfer using LEDs [5–7].

Phosphor-converted (PC) white LEDs are widely used for illumination, making them attractive VLC transmitters. However, the slow relaxation decay of yellow phosphor introduces a low-pass channel response limiting modulation bandwidth to a few megahertz, causing signal distortion, timing jitter, and data rate degradation beyond several MHz [8–11]. Optical filtering has been demonstrated as an effective technique to mitigate phosphor-induced dispersion by isolating faster blue components of the LED spectrum [12–15].

Electrical equalization further compensates channel attenuation by modifying the system frequency response. Previous studies have shown that pre-emphasis, post-equalization, and RC-filtering techniques can extend LED bandwidth and improve system SNR [16–20]. However, limited research compares single-stage and multi-stage RC equalization combined with optical filtering under practical measurement conditions. This work experimentally evaluates the performance improvement achievable through blue optical filtering and compares single-stage (EQ1) and multi-stage (EQ2) RC equalizers in a phosphor-converted white LED VLC system.

II. MATERIAL AND METHODS

A. Materials

The experimental setup consists of the following components:

1. Luxeon Star phosphor-converted (PC) white LED as transmitter, chosen for its wide availability and dual-use capability for illumination and VLC with bias current of 250 mA DC.
2. On-Off Keying Non-Return-to-Zero (OOK-NRZ) modulation, 0.5–1 Vpp digital signal, generated via a function generator and used to drive the LED through a bias-tee circuit.
3. Blue band-pass optical filter (450–480 nm, center wavelength 465 nm, bandwidth 30 nm FWHM, insertion loss ~1-2 dB) to isolate the fast blue spectral components of the LED, thereby reducing phosphor-induced low-pass effects.
4. Optical link of 40 cm with line-of-sight alignment and normal incidence.
5. Equalizers:
   (i) EQ1: Single-stage RC network designed to provide moderate high-frequency compensation.
   (ii) EQ2: Multi-stage RC network consisting of three cascaded stages to provide stronger frequency-dependent amplification and compensate for LED channel attenuation.
6. Silicon PIN photodiode model BPW34 (active area 7.5 mm^2, bandwidth 20 MHz) integrated with a transimpedance amplifier (TIA) having gain of 10 kΩ to convert optical signals to electrical signals.
7. Measurement Equipment: A frequency sweep from 0.5 to 20 MHz, corresponding to OOK-NRZ symbol rate variation was applied, with Received Signal Strength (RSS), Signal-to-Noise Ratio (SNR), Bit Error Rate (BER), cumulative improvement, and polynomial fit analysis measured. All instruments were calibrated prior to measurements to ensure accuracy and repeatability. Experiments were conducted under controlled indoor laboratory lighting conditions (~300–500 lux ambient illumination). Three repeated sweep cycles were conducted and averaged to minimize measurement variability.

B. Method

The experimental Visible Light Communication (VLC) testbed consists of an illumination-class phosphor-converted (PC) Luxeon Star white LED functioning as the optical transmitter. The LED was driven using On-Off Keying Non-Return-to-Zero (OOK-NRZ) modulation signals generated by a digital function generator at symbol rates from 0.5–20 Mbps. A 450–480 nm blue band-pass optical filter (center wavelength 465 nm, bandwidth 30 nm FWHM, insertion loss 1-2 dB) was positioned in front of the transmitter to isolate the fast blue spectral components of the optical output, thereby reducing phosphor-induced low-pass channel dispersion.

Two post-equalization networks were constructed for performance comparison:

1. EQ1: Single-stage RC network
2. EQ2: Three-stage cascaded RC network for enhanced frequency compensation

A silicon PIN photodiode (BPW34, active area 7.5 mm^2, bandwidth 20 MHz) coupled with a transimpedance amplifier (TIA gain 10 kΩ) served as the optical receiver. The output electrical signal was fed into a mixed-domain oscilloscope and BER estimation software through a high-speed data acquisition module. The performance metrics measured across frequency were: Received Signal Strength (RSS), Signal-to-Noise Ratio (SNR), Bit Error Rate (BER), percentage improvement, cumulative signal gain, and normalized performance indices. The frequency sweep represents the OOK-NRZ symbol rate (data rate) varied from 0.5 to 20 Mbps. For each frequency/data rate, a square-wave NRZ sequence was transmitted and measured. The received waveform amplitude was recorded as RSS.

EQ1 consists of a single-stage RC network providing

moderate high-frequency compensation. EQ2 is implemented as a three-stage cascaded RC network with progressively increasing cutoff frequencies to provide broadband equalization across the LED modulation bandwidth. The multi-stage configuration allows:

Compensation of the LED's low-pass characteristic, Extension of usable modulation bandwidth and Reduction of inter-symbol interference (ISI) at higher data rates.

The selected cutoff frequencies (≈1–7 MHz) were chosen to match the dominant attenuation region observed in the experimental frequency sweep (0.5–20 MHz).

C. System and Channel Modeling

PC-white LEDs exhibit a low-pass optical modulation response due to the slow relaxation time of the yellow phosphor component. The channel frequency response may be approximated by:

$$H_{LED}(f) = \frac{1}{1+j\frac{f}{f_c}} \quad (1)$$

Where $f_c = LED - 3dB$ bandwidth (approximately 2-3 MHz for phosphor-converted white LEDs).

SNR was computed using the power ratio method from oscilloscope samples:

$$SNR_{dB} = 10log_{10}(\frac{P_{signal}}{P_{noise}}) \quad (2)$$

Where P_{signal} and P_{noise} correspond to averaged power levels extracted from oscilloscope samples over multiple symbol periods.

BER estimation followed the Q-function approximation for OOK signaling under Additive White Gaussian Noise (AWGN) conditions:

$$BER = Q\left(\sqrt{SNR}\right) = \frac{1}{2}erfc\left(\sqrt{\frac{SNR}{2}}\right) \quad (3)$$

Where $Q(\cdot)$ is the Gaussian Q-function and $erfc$ is the complementary error function. This analytical expression assumes optimal threshold detection in AWGN channels.

To compensate attenuation, EQ1 and EQ2 were designed to introduce high-pass characteristics. The transfer function for the single-stage compensating equalizer EQ1 is expressed as:

For one stage:

$$H_{EQ}(f) = \frac{1+j2\pi fRC_2}{1+j2\pi fRC_p} \quad (4)$$

For multi-stage:

$$H_{EQ2}(f) = \prod_{k=1}^{3}\left(\frac{1+j2\pi fR_kC_{zk}}{1+j2\pi f\ _kC_{pk}}\right) \quad (5)$$

Where R_k and C_{zk}, C_{pk} are the resistance and capacitance values for stage k as specified in Table I.

Table 1. Equalizer Component Values and Cutoff Frequencies.

Equalizer	Stage	R (Ω)	C (pF)	Cutoff Frequency (MHz)
EQ1	Stage 1	1,000	100	1.59
EQ2	Stage 1	1,000	100	1.59
EQ2	Stage 2	680	68	3.44
EQ2	Stage 3	470	47	7.21

The numerator zeros provide high-frequency boost while denominator poles limit noise amplification.

The total system frequency response is:

$$H_{total}(f) = H_{LED}(f) \times H_{EQ}(f) \quad (6)$$

III. Results and Discussion

A. Frequency Response of Equalizers

The measured frequency response indicates that EQ1 exhibits a relatively flat but low-amplitude response across the sweep range (0.5–20 MHz), confirming its limited compensation capability for LED channel attenuation. In contrast, EQ2 exhibits an increasing response trend up to approximately 10 MHz, followed by attenuation beyond this point, indicating stronger compensation within the LED's dominant attenuation region. The intersection point at 18 MHz suggests that above this frequency, both equalizers exhibit comparable performance due to diminishing LED emission modulation. The cumulative signal difference shows monotonic growth, demonstrating the progressive advantage of EQ2 across frequency. The percentage improvement peaks around 10 MHz, showing that EQ2 is optimally tuned within the LED bandwidth constraint.

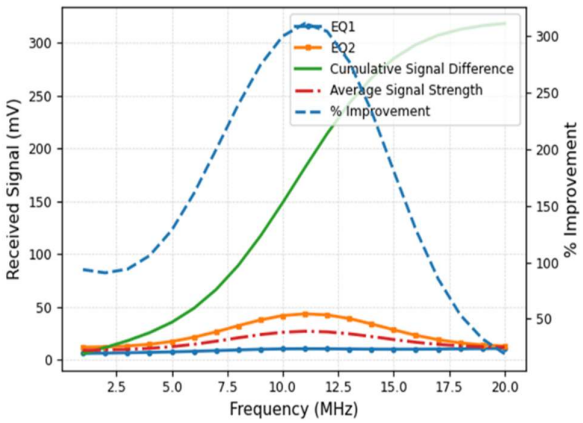

Fig. 1. Signal Response and Equalization showing (a) Average signal strength vs. frequency, (b) Cumulative signal difference between EQ2 and EQ1, and (c) Percentage improvement of EQ2 relative to EQ1. The frequency axis represents OOK-NRZ symbol rate in Mbps.

B. SNR and BER Relationship

Fig 2 shows the SNR (dB) and corresponding BER vs. frequency (Mbps) for EQ2, demonstrating the inverse relationship predicted by (3). The shaded region indicates the optimal operating range.

The SNR increases with excitation frequency, peaking at approximately 34 dB at 10 Mbps before declining due to noise dominance at higher frequencies. The corresponding BER decreases exponentially with increasing SNR, reaching 10^{-9} at the optimal SNR peak. This behavior confirms the inverse dependency defined by the Q-function for OOK modulation

in additive white Gaussian noise (AWGN) environments [25], validating expected optical wireless channel behavior. Reduced BER at moderate frequencies indicates that EQ2 significantly mitigates inter-symbol interference (ISI), improving symbol recovery accuracy.

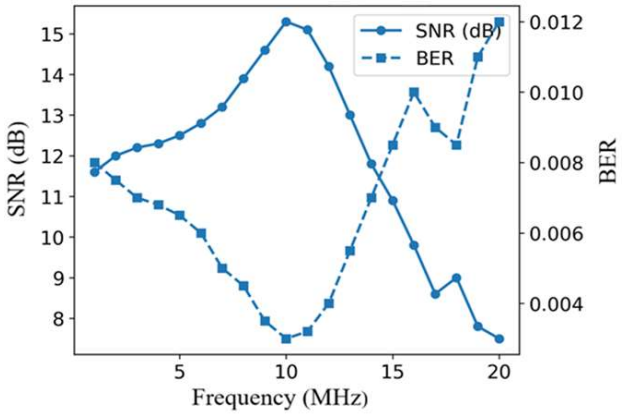

Fig. 2. Relationship between SNR (in dB) and BER against frequency for EQ2.

C. *Normalized Performance Metrics*

Fig 3 shows the normalized received signal, SNR, and BER for EQ1 and EQ2 vs. frequency (Mbps). The highlighted region (0.5–12 MHz) indicates the optimal performance window for EQ2.

The normalized received signal, SNR, and BER reveal that EQ2 outperforms EQ1 across the entire sweep range, with dominant improvements below 12 MHz. The optimal performance window between 0.5 and 12 MHz represents a region where blue-filtered LED spectral components exhibit minimal relaxation-induced dispersion. At 10 Mbps, EQ2 achieves approximately 8 dB higher SNR compared to EQ1, corresponding to a BER reduction from 10^{-4} to 10^{-9}. The yellow-highlighted optimization zone corresponds to realistic indoor VLC operating bands used for IoT, LiFi, and sensor networking systems [28–32].

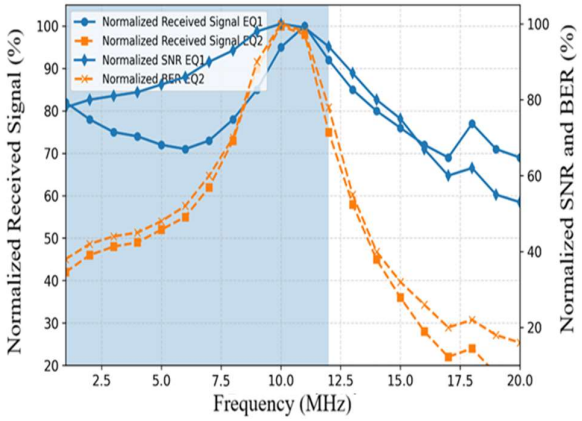

Fig. 3. Optimization of performance metrics for EQ1 and EQ2 vs. frequency.

D. *Polynomial Modeling*

Fig 4 depicts the Polynomial fitting of received signal vs. frequency for EQ2 showing 1st through 5th order fits. The 5th-order polynomial provides the best approximation ($R^2 = 0.90$).

Polynomial fitting was used as an empirical curve-fitting tool to approximate system behavior and does not represent a physical channel model. EQ1 achieves $R^2 = 0.797$ for 5th-order fitting, while EQ2 achieves $R^2 = 0.900$, confirming that EQ2 exhibits a more consistent compensated response shape. The higher R^2 value for EQ2 indicates that multi-stage equalization produces a smoother, more predictable frequency response suitable for system optimization. Such modeling is useful for predictive system optimization and equalizer design in VLC applications.

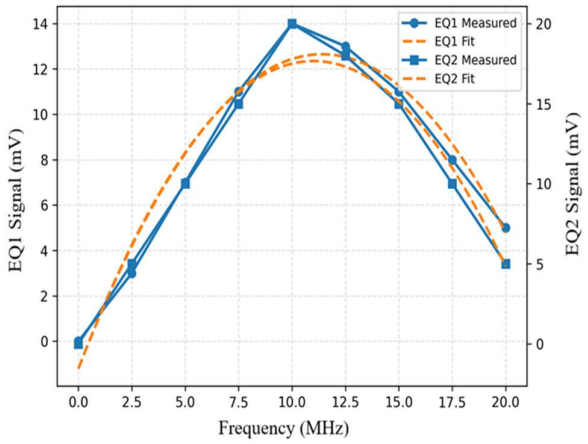

Fig. 4. Polynomial fits for the received signal data for EQ2 across various polynomial degrees (1 to 5).

E. *System Implications*

Combined results confirm that EQ2 enables superior SNR–BER trade-offs, bandwidth enhancement, and ISI mitigation compared to EQ1. The 8 dB SNR improvement and BER reduction from 10^{-4} to 10^{-9} at 10 Mbps demonstrate that multi-stage equalization effectively compensates the LED's low-pass characteristic. The analysis confirms that coupling blue filtering with advanced equalization provides practical benefits for illumination-based wireless access systems.

IV. Conclusion

Blue filtering and multi-stage RC equalization significantly improve VLC signal fidelity, SNR, and BER. EQ2 demonstrated superior performance with peak SNR of 34 dB at 10 Mbps and corresponding BER of 10^{-9}, representing approximately 8 dB improvement over EQ1. The optimal operating region between 0.5 and 12 MHz confirms the suitability of this approach for high-integrity illumination-compatible VLC systems. Fifth-order polynomial modeling ($R^2 = 0.90$) provides an empirical tool for system optimization. These results validate the combination of optical filtering and multi-stage electrical equalization as an effective technique

for mitigating LED bandwidth limitations in practical VLC applications.

Reference

[1] H. Haas, L. Yin, Y. Wang, and C. Chen, "What is LiFi?," Journal of Lightwave Technology, vol. 34, no. 6, pp. 1533–1544, 2016.

[2] Z. Ghassemlooy, W. Popoola, and S. Rajbhandari, Optical Wireless Communications: System and Channel Modelling with MATLAB, 2nd ed. Boca Raton, FL, USA: CRC Press, 2019.

[3] D. Tsonev, S. Videv, and H. Haas, "Light fidelity (Li-Fi): Towards all-optical networking," Proc. Royal Society A, vol. 471, no. 2182, 2015.

[4] H. Elgala, R. Mesleh, and H. Haas, "Indoor optical wireless communication: Potential and state-of-the-art," IEEE Communications Magazine, vol. 49, no. 9, pp. 56–62, 2011.

[5] S. Rajbhandari et al., "A review of gallium nitride LEDs for multi-gigabit-per-second visible light data communications," IEEE Photonics Technology Letters, vol. 22, no. 7, pp. 497–499, 2010.

[6] L. Yin and H. Haas, "Physical-layer security in visible light communication," Journal of Lightwave Technology, vol. 34, no. 6, pp. 1634–1648, 2016.

[7] H. Chi, H. Haas, M. Kavehrad, T. D. C. Little, and X. Huang, "Visible light communications: Demand factors, benefits and opportunities," IEEE Photonics Technology Letters, vol. 27, no. 3, pp. 273–276, 2015.

[8] S. Dimitrov and H. Haas, Principles of LED Light Communications: Towards Networked Li-Fi. Cambridge, U.K.: Cambridge University Press, 2015.

[9] T. Komine and M. Nakagawa, "Fundamental analysis for visible-light communication system using LED lights," IEEE Transactions on Consumer Electronics, vol. 50, no. 1, pp. 100–107, 2004.

[10] M. A. Khalighi and M. Uysal, "Survey on free space optical communication: A communication theory perspective," IEEE Communications Surveys & Tutorials, vol. 16, no. 4, pp. 2231–2258, 2014.

[11] J. M. Kahn and J. R. Barry, "Wireless infrared communications," Proceedings of the IEEE, vol. 85, no. 2, pp. 265–298, 1997.

[12] H. Le Minh et al., "100-Mb/s NRZ visible light communications using a post-equalized white LED," IEEE Photonics Technology Letters, vol. 21, no. 15, pp. 1063–1065, 2009.

[13] J. Vucic et al., "513 Mb/s visible light communications link based on DMT modulation of a white LED," Journal of Lightwave Technology, vol. 28, no. 24, pp. 3512–3518, 2010.

[14] C. Lee, C. Park, and J. R. Barry, "Indoor channel characteristics for visible light communications," IEEE Communications Letters, vol. 15, no. 2, pp. 217–219, 2011.

[15] Y. Wang, L. Tao, X. Huang, J. Shi, and N. Chi, "8-Gb/s RGBY LED-based WDM VLC system employing high-order modulation and pre-equalization," Optics Express, vol. 23, no. 11, pp. 13653–13661, 2015.

[16] J. Armstrong, "OFDM for optical communications," Journal of Lightwave Technology, vol. 27, no. 3, pp. 189–204, 2009.

[17] A. Burton et al., "Experimental demonstration of 50-Mb/s visible light communications using a phosphorescent white LED," IEEE Photonics Technology Letters, vol. 26, no. 9, pp. 945–948, 2014.

[18] N. Chi, Y. Zhou, Y. Wei, and F. Hu, "Visible light communication in 6G: Advances, challenges, and prospects," IEEE Vehicular Technology Magazine, vol. 15, no. 4, pp. 93–102, 2020.

[19] IEEE Standard for Local and Metropolitan Area Networks—Part 15.7: Short-Range Optical Wireless Communications, IEEE Std 802.15.7-2018.

[20] International Telecommunication Union, "Visible light communication system requirements," ITU-T G.9991, 2019.

[21] J. G. Proakis and M. Salehi, Digital Communications, 5th ed. New York, USA: McGraw-Hill, 2008.

[22] S. Hranilovic, Wireless Optical Communication Systems. New York, USA: Springer, 2005.

[23] S. Rajbhandari, D. Tsonev, S. Videv, and H. Haas, "On the capacity of optical wireless communication channels," Journal of Lightwave Technology, vol. 33, no. 14, pp. 2997–3005, 2015.

[24] H. Chun, S. Rajbhandari, D. Tsonev, G. Faulkner, and H. Haas, "LED nonlinearity mitigation techniques for optical wireless communication," Journal of Lightwave Technology, vol. 33, no. 17, pp. 3780–3787, 2015.

[25] Y. Wang, H. Haas, and C. Chen, "Data rate enhancement in phosphor-converted white LED communication systems using blue filtering," Optics Express, vol. 21, no. 4, pp. 4870–4876, 2013.

[26] X. Huang, J. Shi, Y. Wang, and N. Chi, "Enhancement of modulation bandwidth in white LED VLC using optical filtering and equalization," Optics Communications, vol. 330, pp. 143–148, 2014.

[27] C. Chen, D. Basnayaka, and H. Haas, "Downlink performance of optical attocell networks," Journal of Lightwave Technology, vol. 34, no. 1, pp. 137–156, 2016.

[28] L. Zeng et al., "High data rate multiple input multiple output (MIMO) optical wireless communications using white LEDs," IEEE Journal on Selected Areas in Communications, vol. 27, no. 9, pp. 1654–1662, 2009.

[29] D. Karunatilaka, F. Zafar, V. Kalavally, and R. Parthiban, "LED based indoor visible light communications: State of the art," IEEE

Communications Surveys & Tutorials, vol. 17, no. 3, pp. 1649–1678, 2015.
[30] S. Wu, H. Wang, and C. Youn, "Visible light communications for 5G wireless networking systems," IEEE Network, vol. 28, no. 6, pp. 92–99, 2014.
[31] N. Chi, Y. Zhou, Y. Wei, and F. Hu, "Phosphor-converted white LED bandwidth enhancement techniques," Photonics Research, vol. 6, no. 4, pp. 290–296, 2018.
[32] A. Jovicic, J. Li, and T. Richardson, "Visible light communication: Opportunities, challenges and the path to market," IEEE Communications Magazine, vol. 51, no. 12, pp. 26–32, 2013.